International Journal of Multidisciplinary Research and Growth Evaluation.

Geology of Karanggayam Village and Surrounding Areas, Karanggayam Subdistrict, Kebumen Regency, Central Java Province

Mohamad Salsabila [1], Surya Darma Hafiz [2*], Dyah Ayu Setyorini [3], Wildan Tri Koesmawardani [4], Himmes Fitra Yuda [5], Novi Triany [6]

[1] Student at Program Studi Magister Teknik Geologi, Fakultas Teknologi Kebumian dan Energi, Universitas Trisakti, Jakarta, Indonesia.

[2-6] Lecturer at Program Studi Sarjana Teknik Geologi, Fakultas Teknologi Kebumian dan Energi, Universitas Trisakti, Jakarta, Indonesia

* Corresponding Author: **Surya Darma Hafiz**

Article Info

ISSN (Online): 2582-7138
Impact Factor (RSIF): 7.98
Volume: 06
Issue: 05
September - October 2025
Received: 30-06-2025
Accepted: 28-07-2025
Published: 12-09-2025
Page No: 42-56

Abstract

Indonesia is located at the confluence of three tectonic plates, namely the Australian Plate, the Eurasian Plate and the Pacific Plate. Plate movements make Indonesia traversed by a volcanic route or the Ring of Fire which results in Indonesia having a complex geological condition. Therefore, Indonesia is one of the best countries to conduct a geological mapping study. One area in Indonesia that has a good geological condition is in the area of Karanggayam Village, Karanggayam District, Kebumen Regency, and Central Java Province. The method used is primary data collection in the form of geological data searches, observations of geomorphological phenomena and processes and field data analysis. From this method, the geomorphology of the research area is divided into six geomorphological units. And the constituent lithology consists of four lithostrate rock units and 1 lithodemic, among others from old to young, namely fragmented claystone units, monomic breccias, diabase intrusions, sandstones alternating with claystones and carbonated sandstones. The geological structure in the mapping area is in the form of folds such as anticlines and synclines and faults in the form of descending, ascending and horizontally sinistral faults. Geological history that occurs in the mapping area is estimated to have occurred during the early Miocene to late Miocene and was deposited from a submarine fan environment. Geological evaluation in the mapping area is in the form of natural resource potential in the form of natural tourism mining mines, as well as geological disaster constraints in this area such as ground movement that triggers landslides.

Keywords: Geology, Micropaleontology, Karangduwet, Geological History, Gunungkidul

1. Introduction

Geology is a fundamental science essential for understanding the Earth's condition. Through geological knowledge, humans can comprehend Earth's structure, constituent materials, and geological processes that shape the current state of the planet. Due to dynamic geological processes, each region on Earth possesses unique geological characteristics. These can be identified through geological mapping activities, which are crucial for applications such as natural resource exploration and hazard assessment to support sustainable land use planning.

In general, geological mapping involves collecting data and field-based information regarding the distribution of rocks, structural features, and surface morphology within a specific area. Although previous geological mappings have been conducted in the research area, these were performed at a regional scale, rendering them less detailed and inadequate in identifying smaller geological features. Hence, this study employs a more detailed scale of 1:12,500, aiming to achieve higher-resolution and representative mapping outcomes.

This enables identification of both the potential resources and geological hazards within the region. Karanggayam Village and its surroundings, particularly within Karanggayam Subdistrict, Kebumen Regency, are of special geological interest. This mapping aims to refine the lithological classification of the area. The region is structurally controlled by geological structures such as faults and folds, necessitating a study of geological hazard mitigation. Furthermore, the area's natural resource potential could be harnessed for the benefit of local communities.

Regional Geology

Geographically, the mapping area lies between 109°32′30.6996″ – 109°34′41.1672″ E and 7°33′50.0508″ – 7°36′33.5844″ S. Administratively, it is located in Karanggayam Subdistrict, Kebumen Regency, Central Java Province, covering Karanggayam, Pohkumbang, Penimbun, and Karangmojo Villages (Figure 1.1). The study area spans 20 km², with approximate dimensions of 5 km by 4 km.

Previous investigations of the area have been carried out by earlier researchers. Van Bemmelen (1994), in The Geology of Indonesia, divided Central Java into several physiographic zones: the North Java Alluvial Plain, the Bogor Anticlinorium (consisting of the Northern Serayu Mountains and Kendeng Range), the Central Java Depression Zone, the Southern Serayu Mountains, the Southern Mountains of West and East Java, and Quaternary volcanic regions.

The study area falls within the Kebumen Sheet of the regional geological map. According to Asikin *et al.* (1992) [1], the stratigraphic succession from oldest to youngest includes:

1. Karangsambung Formation: Composed of gray claystone with iron concretions, Nummulitic limestone, conglomerates, and laminated polymict quartz sandstone. The presence of graywacke sandstone and black shale exhibiting fissile structures indicates large-scale submarine deposition. This formation is dated Middle to Late Eocene based on planktonic foraminifera.
2. Waturanda Formation: Consists of volcanic breccia, sandstone, and claystone containing feldspar, pyroxene, clay, and lithic fragments. The upper part includes andesitic and basaltic breccias with calcareous tuff. The presence of planktonic foraminifera suggests an Early to Middle Miocene age, deposited in a deep marine proximal turbidite setting forming elevated morphology.
3. Penosogan Formation: Interbedded sandstone, claystone, tuff, marl, and calcarenite with thicknesses ranging from 5–60 cm. Calcarenites contain foraminifera and coral fragments, while marl interbeds contain both larger and smaller foraminifera. This formation is Middle Miocene in age, deposited in an upper bathyal environment through proximal to distal turbidite flows.
4. Halang Formation: Comprises alternating sandstone, claystone, marl, tuff, and breccia interbeds. The strata exhibit graded bedding and parallel lamination. Planktonic foraminifera indicate a Middle Miocene to Early Pliocene age. Depositional settings range from shallow to open marine (neritic), with paleocurrent directions toward the southeast and southwest.

2. Methodology

The research employed a combination of surface mapping, descriptive analysis, and laboratory investigations. The stages included preparation and planning, fieldwork, laboratory analysis, and report compilation.

A. Preparation and Planning :

1. Literature Review: Assessing the geological context based on previous studies.
2. Traverse Planning: Designing efficient and effective traverses, particularly those perpendicular to bedding strikes and crossing rivers.
3. Topographic Map Analysis: Creating drainage pattern maps to predict geological structures.
4. Equipment Preparation: Compiling necessary tools, including topographic maps, a geological compass, rock sampling tools, GPS, and field notebooks.

B. Fieldwork :

1. Observation Sites: Determining observation points and plotting them with GPS.
2. Measurements and Observations: Utilizing geological compasses, hammers, HCl solution, magnifiers, and comparators to record lithological and structural data (e.g., strike, dip, bedding, and faults).
3. Data Recording: Documenting observations in field notebooks and photographing outcrops.

C. Laboratory Analysis:

1. Petrographic Analysis: Microscopic examination of thin sections to determine rock facies.
2. Micropaleontological Analysis: Identifying foraminifera fossils to establish relative ages and depositional environments.
3. Stratigraphic Analysis: Determining thicknesses and sequences of stratigraphic units.
4. Structural Analysis: Interpreting structural patterns and tectonic stresses.
5. Calcimetry: Measuring $CaCO_3$ content in rock samples.

D. Report Compilation:

Field and laboratory results were integrated into a comprehensive geological report, supervised and reviewed in consultation with academic advisors. Previous works, such as Van Bemmelen (1994) and the Kebumen Sheet Geological Map (Asikin *et al*., 1992) [1], were also consulted to support the regional geological interpretation.

3. Result and Discussion

Field mapping data were categorized into geomorphological, lithological, and structural observations. Investigations were conducted along riverbanks, riverbeds (where faults were evident), road cuts, and cliff faces formed by landslides. The observation map is presented in Figure 1.

Stratigraphic interpretation was based on dominant lithological features within informal rock units, delineated using a 1:12,500 topographic map and applying the law of V-shaped valley topography. Contacts between units were only observed in limited locations, owing to weathering and soil cover. Therefore, topography and bedding orientation were considered in determining unit boundaries.

The age and bathymetry of the stratigraphic units were determined using two approaches:\

1. Steno's Law of Superposition and cross-sectional reconstruction.
2. Foraminiferal Analysis, both planktonic (Blow, 1969) and benthonic (Bandy, 1967), with depositional

environment interpreted through the submarine fan model of Walker (1978) [16].

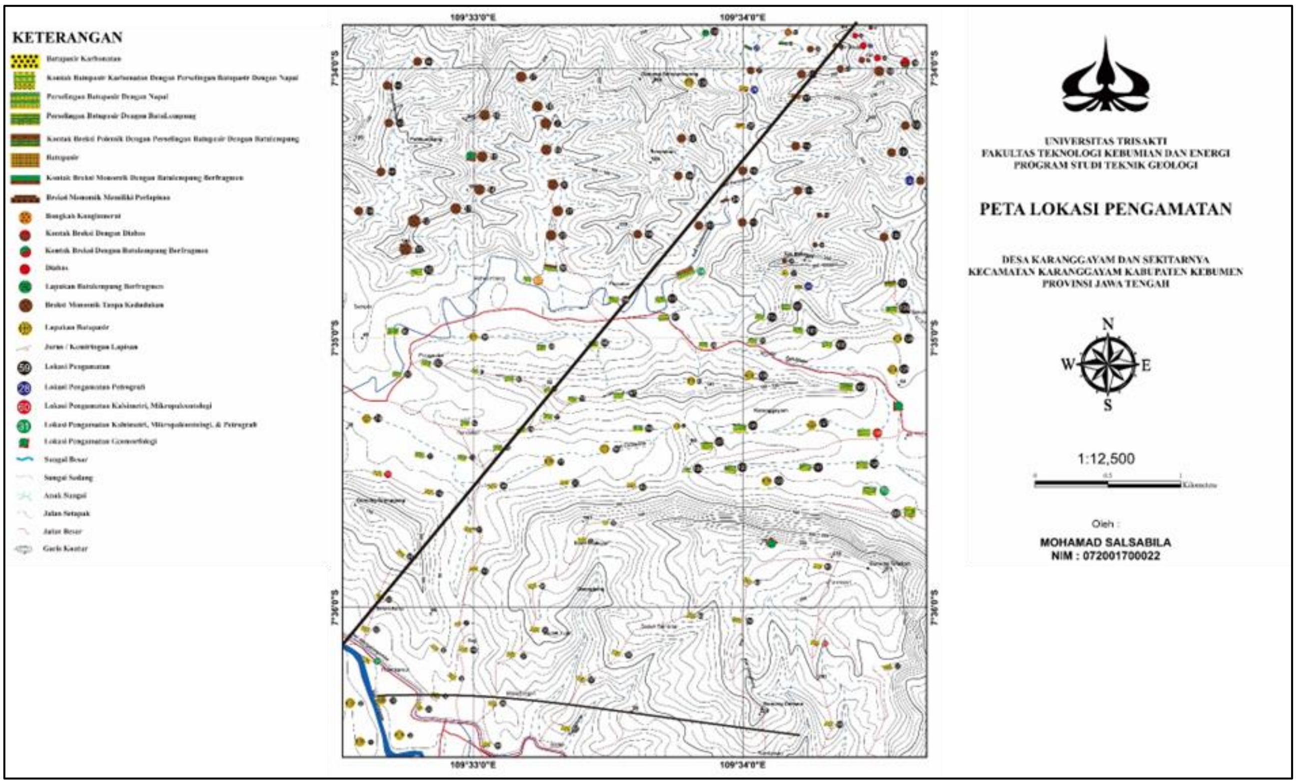

Fig 1: Observation Location Map

Based on these observations, the rock units in the study area can be stratigraphically ordered from oldest to youngest as follows (Figure 2). The Fragmented Claystone Unit occupies approximately ±5% of the mapping area in the northern part of the map, with an east–west distribution covering the Penimbun and Sempudoyong villages. The estimated thickness of this unit, based on geological cross-section calculations, reaches approximately ±291 meters. Macroscopically, the rocks are found in weathered to fresh conditions at various locations. This unit is characterized by a gray to glossy clay-sized matrix with non-carbonate cement and contains lithic fragments, quartz, and basaltic igneous rock fragments ranging from 4 mm to <40 mm (gravel–pebble size) that are sub-rounded in shape. The unit exhibits poor compaction and generally lacks visible bedding, although at location point LP 28, a contact with the overlying Monomictic Breccia Unit is interpreted.

Microscopically, the Fragmented Claystone (Figure 3) shows a massive texture with grain sizes ranging from 1/256 mm to 1/16 mm, good sorting, and closed packing. Thin section analysis reveals mineral composition as follows: Quartz (distributed in A6), Siliceous Clay Minerals (in B6), Oxidized Clay Minerals (in G10), and Opaque Minerals (in F2). According to Pettijohn's (1975) classification, this sample is categorized as Mudrock.

Overlying this unit is the Monomictic Breccia Unit, which covers approximately ±40% of the northern mapping area, extending in an east–west direction across the Pohkumbang, Penimbun, and Karangmojo regions. Outcrop conditions range from fresh to weathered. Based on cross-sectional estimation, the thickness of this unit reaches up to ±782 meters.

From a macroscopic perspective, the lower part of this unit consists of Monomictic Breccia interbedded with sandstone. The Monomictic Breccia appears black to gray in color, with sub-angular clasts ranging in size from gravel to boulder, poorly sorted, open-packed, and composed predominantly of andesitic igneous rock fragments. These fragments are gray in color, exhibit hypocrystalline textures, aphanitic grain size, subhedral crystal habit, inequigranular fabric, and display graded bedding structures.

In the middle part of the unit, gray-colored sandstone interbeds are observed, with alternating very coarse to fine grains, poorly sorted, closed-packed, and cemented by non-carbonate materials containing quartz, pyroxene, and feldspar minerals.

Higher up in the sequence, Monomictic Breccia becomes more layered and progressively coarser. Macroscopically, this breccia contains gravel to boulder-sized angular to sub-angular clasts, grain-supported with moderate compaction. Its mineral composition includes plagioclase, pyroxene, and quartz. The igneous fragments appear gray to black, exhibit crystalline structure, phaneritic granularity, inequigranular texture, and massive fabric—typical characteristics of andesite.

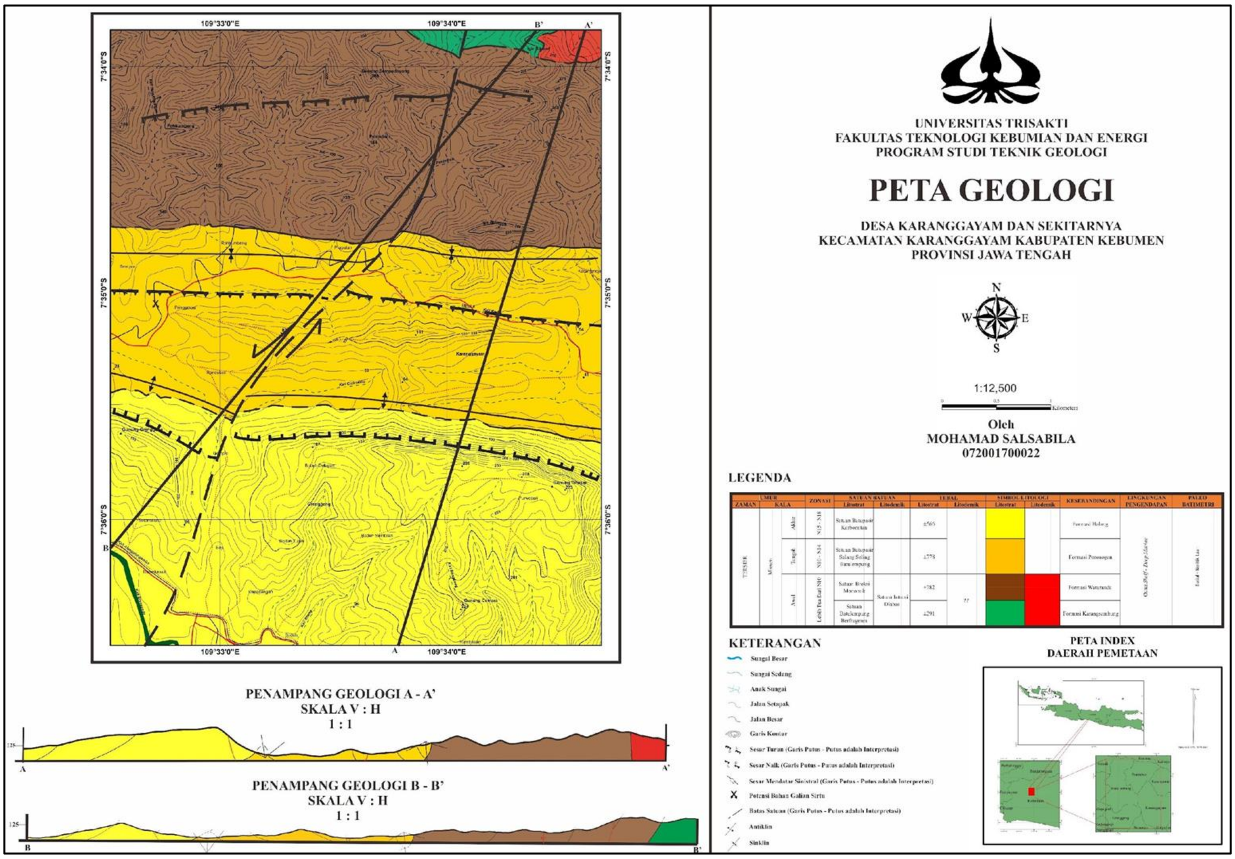

Fig 2: Geological map of the study area

At the top of the unit, sandstone beds gradually transition into Polymictic Breccia, which contains igneous rock fragments, lithic components, and crystalline limestone fragments. Macroscopically, the Polymictic Breccia contains angular to sub-angular gravel–boulder-sized clasts, grain-supported, poorly sorted, and moderately compacted. The matrix ranges from medium to coarse sandstone. The mineral composition includes plagioclase, pyroxene, opaque minerals, and volcanic glass. The igneous rock fragments are black in color, hypocrystalline in texture, phaneritic in granularity, inequigranular in texture, and massive in fabric—indicating andesitic composition. Limestone fragments are white and display crystalline textures.

The interbedded sandstone is gray, with alternating very coarse to fine grain sizes, poorly sorted, mud-supported, cemented with non-carbonate material, and contains quartz and feldspar minerals.

Microscopically (Figure 4), the Monomictic Breccia features andesitic fragments with hypocrystalline, inequigranular textures and phenocrysts ranging in size from ¼ to 1 mm, showing hypidiomorphic crystal shapes. The thin section reveals mineral composition including plagioclase (observed at E-10), orthopyroxene (C-4), and opaque minerals (B4). The matrix of this Monomictic Breccia unit, however, could not be analyzed petrographically due to its condition.

An intrusion that cuts through the Monomictic Breccia Unit is observed in the field, which is not found in any other rock units in the study area. Macroscopically, this intrusive body occupies approximately ±3% of the mapped area, specifically in the northeastern section near Igir Sikaret, Penimbun. The unit is situated at the highest contour elevation in the mapping area, and the outcrop predominantly displays weathered rock. In general, from a macroscopic perspective, the unit is classified as an intermediate igneous rock. The localized weathering is interpreted to result from contact metamorphism or thermal alteration with adjacent units. The fresh surface color tends to be gray, while the weathered surface is relatively brown. It exhibits hypocrystalline texture, phaneritic granularity, subhedral crystal form, inequigranular texture, and identifiable minerals. Diabasic structures are also visible, indicating characteristics of diabase rocks. However, due to weathering and uncertainty in macroscopic observations, microscopic analysis is required for accurate classification.

Microscopically (Figure 7), the diabase intrusion unit shows a massive texture with aphanitic granularity and fine-to-medium mineral grain size (1–5 mm). Several minerals are identified under the microscope: plagioclase with an abundance of 50%, occurring as phenocrysts (E5); quartz present in minor amounts (1%) observed at D3; and clinopyroxene with an abundance of 4%, exhibiting a spotted appearance (A10). Based on microscopic analysis, this diabase intrusion unit is classified as Andesite (O'DUNN & SILL, 1986).

Then overlying it is the Interbedded Sandstone–Claystone Unit, which covers approximately ±20% of the mapped area in the central part of the field, with an east–west distribution pattern including the regions of Karanggayam, Pringamba, Karangmojo, and Pohkumbang. The outcrops of this rock unit range from weathered to fresh. The estimated thickness of this unit from cross-sections reaches ±778 meters.

Macroscopically, the lower part of this unit consists of interbedded sandstone–claystone, with a yellowish-brown color. The carbonate sandstone is fine-grained, well-rounded, has a closed packing texture, good sorting, moderate compaction, and is cemented by carbonate. The mineral composition includes feldspar and quartz and exhibits tuffaceous characteristics. Meanwhile, the claystone is dark gray in color, clay-sized, contains carbonate cement, and has a carbonate content of approximately ±6% based on calcimetry. Sedimentary structures observed in this section include parallel and wavy laminations in the sandstone lithology, with scour marks observed at the base.

In the middle part of the unit, the carbonate sandstone is medium to coarse-grained, well-rounded, has closed packing, good sorting, strong compaction, and carbonate cement, also with tuffaceous characteristics. The carbonate claystone is clay-sized with carbonate cement and shows a calcimetry-based carbonate content of ±12%, and also displays tuffaceous characteristics. The only observable sedimentary structure in this section is parallel lamination, and in some places, rip-up clast structures are present. The upper part of the unit contains claystone interbedded with sandstone, having the same lithological characteristics as the middle unit, with the difference being that in the upper part, the carbonate claystone tends to be thicker and has a carbonate content of ±11% according to calcimetry (Table 3.6). Microscopically (Figure 5), the carbonate sandstone is classified as Calcareous Feldspathic Wacke (Modified from Pettijohn, 1975), described as having a massive structure and a grain size ranging from <1/256 to 1/2 mm, with both closed and open packing and good sorting. The thin section consists of Quartz (at A-1), Feldspar (at C9), Carbonate-Clay Minerals (at I1), and Opaque Minerals (at A10) (Appendix 3). Meanwhile, the carbonate claystone is microscopically described as Calcareous Mudrock (Modified from Pettijohn, 1975) with a massive structure, grain size <1/256 to 1/32 mm, good sorting, and closed packing.

The youngest deposit is the Carbonate Sandstone Unit, which covers approximately ±30% of the mapped area in the southern part of the field, with an east–west distribution pattern that includes the regions of Mt. Grenggeng, Mt. Cemara, and Mt. Tutukan. The outcrop condition of this rock unit ranges from weathered to fresh. The estimated thickness of the Carbonate Sandstone Unit from cross-sections reaches ±566 meters. Macroscopically, the lower part of this unit is dominated by yellowish-brown Carbonate Sandstone. It is coarse to medium-grained, sub-rounded in grain shape, mud-supported in fabric, moderately sorted, with moderate compaction, and cemented by carbonate, having a carbonate content of approximately ±13%. The fragments consist of lithic mudrock, and the mineral composition includes feldspar and quartz. This lower section shows a massive structure.

Toward the middle part, the Carbonate Sandstone contains larger lithic mudrock fragments, ranging from 1 mm to 2 mm in size. It is medium to coarse-grained, rounded in grain shape, grain-supported, moderately sorted, moderately compacted, and cemented by carbonate with a carbonate content of approximately ±10%. The fragments consist of lithics and pyroclastic rocks. The mineral composition, still dominated by feldspar and quartz, is similar to the previous section. Starting from the middle part, sedimentary structures such as parallel lamination and rip-up mudrock structures are visible.

In the upper part, the Carbonate Sandstone is light brown in color, coarse-grained, rounded in grain shape, grain-supported, moderately sorted, and moderately compacted. The fragments consist of lithic mudrock ranging from 10 to 19 mm in size, cemented by carbonate with a carbonate content of 15%. The mineral composition includes plagioclase, hornblende, and minor quartz. Sedimentary structures observed in this section include parallel lamination and rip-up mudrock structures. Microscopically (Figure 6), this Carbonate Sandstone is classified as Calcareous Lithic Wacke (Modified from Pettijohn, 1975). It is described as having a massive structure, with grain sizes ranging from <1/256 to 1/6 mm, both closed and open packing, and good sorting. The thin section composition includes:

Carbonate–clay minerals: 69% distributed throughout, Quartz: 1% abundance, observed at A8, Feldspar: 3% abundance, observed at E5.

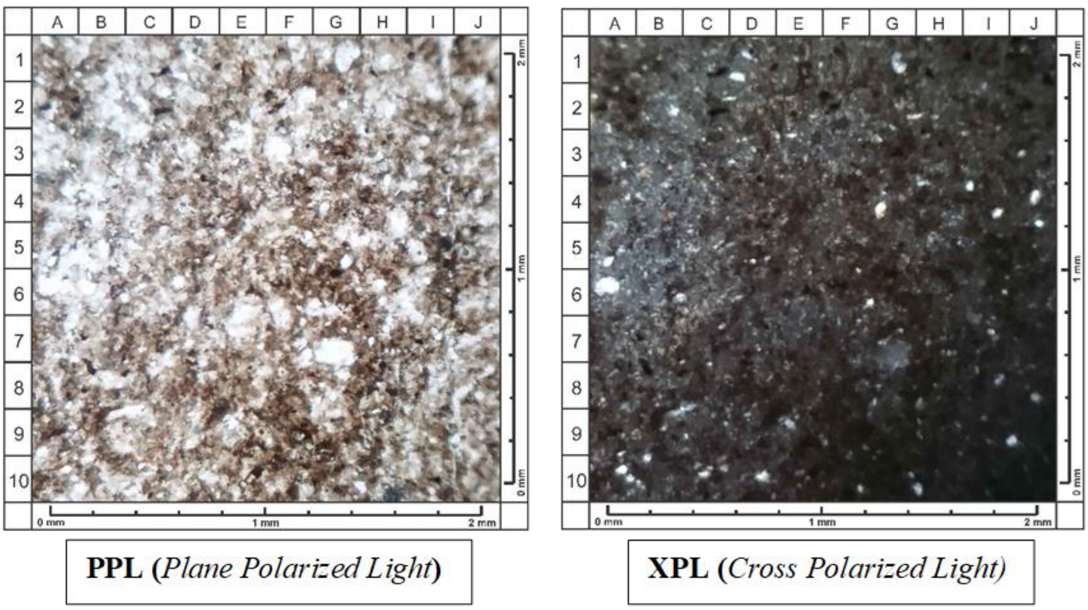

Fig 3: The appearance of the thin section at observation location 28 (Fragmented Claystone Unit)

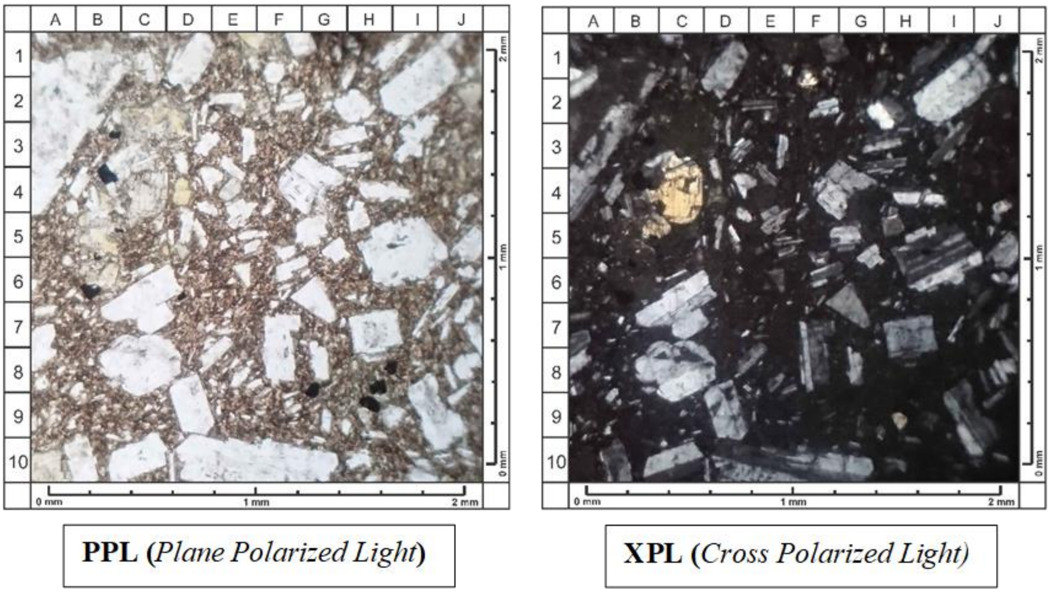

Fig 4: The appearance of the thin section at observation location 133 (Monomict Breccia Unit Fragment)

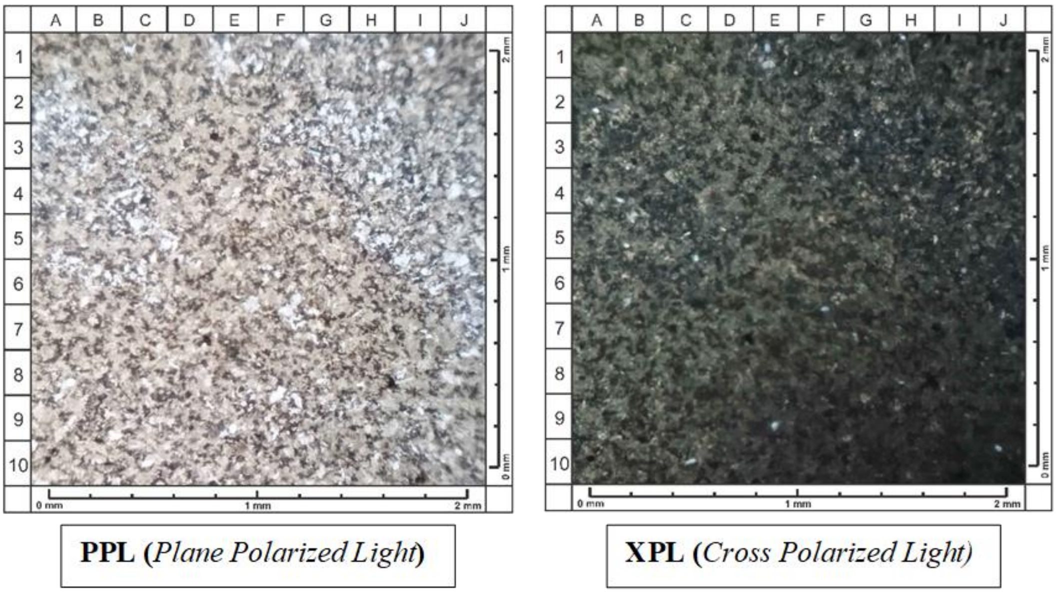

Fig 5: The appearance of the thin section at observation location 70 (Interbedded Sandstone–Claystone Unit)

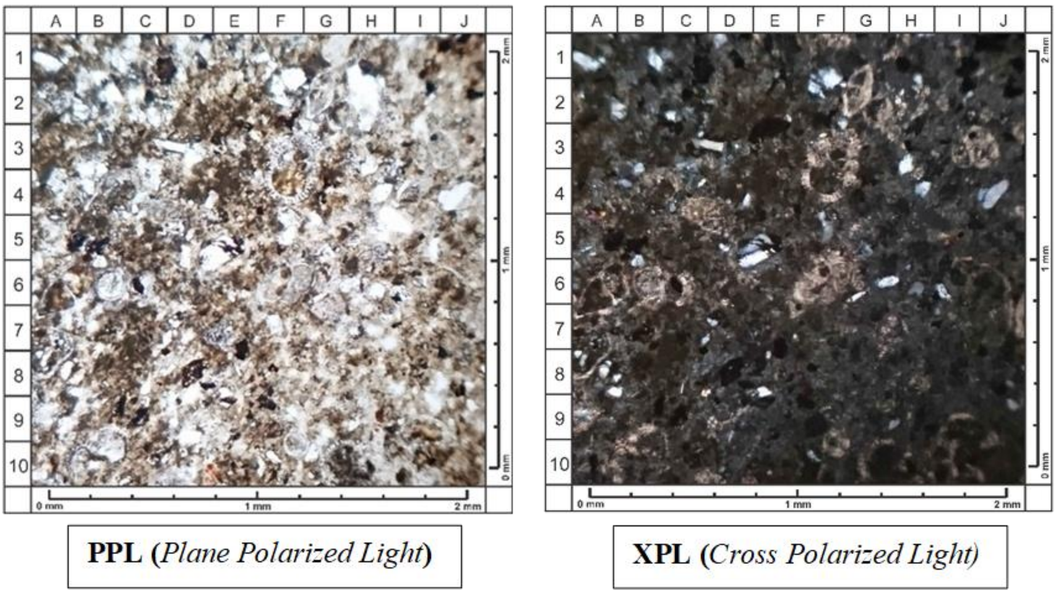

Fig 6: The appearance of the thin section at observation location 31 (Carbonate Sandstone Unit)

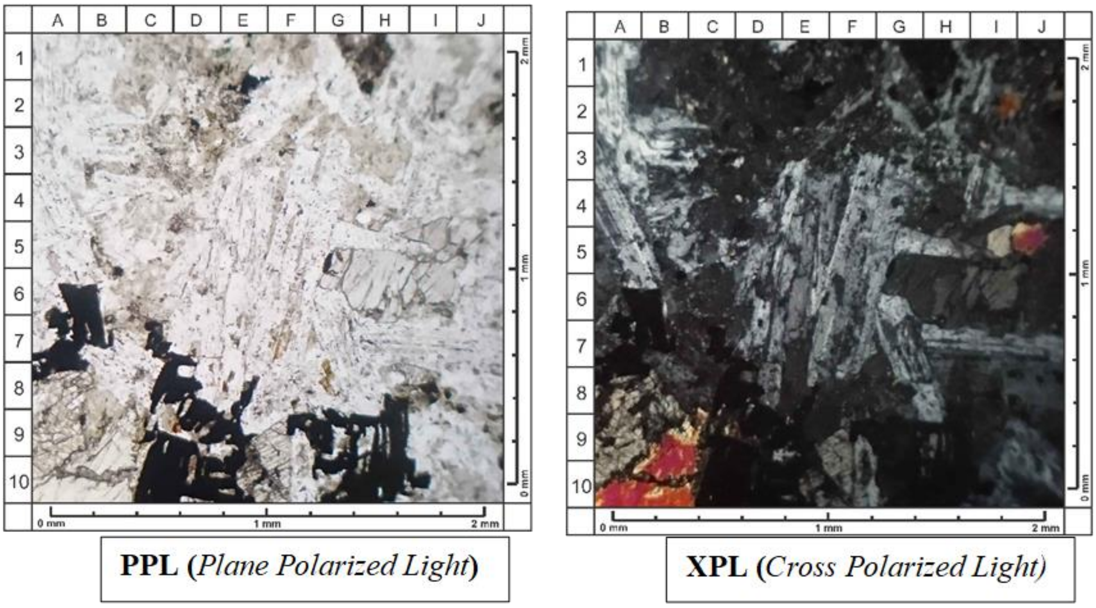

Fig 7: The appearance of the thin section at observation location 48 ST1 (Diabase Intrusion Unit)

Determination of Rock Unit Age

The age determination of rock units is carried out using cross-sectional profiles and the sequence of reconstructed geological history, as well as fossil data that have been identified. Therefore, even rock units that lack fossil data can have their ages estimated based on stratigraphic relationships, lithological reconstruction, and literature review.

For the Fragmented Claystone Unit, age determination cannot rely on fossil content due to the results of microfossil analysis being barren. Thus, the age of this unit is determined based on stratigraphic relationships, lithological reconstruction, and reference studies, indicating that it is older than the Monomict Breccia Unit.

As shown in Table 1, the age of the Monomict Breccia Unit, based on fossil analysis, indicates it is older than N10.

Based on the cross-sectional profile and the reconstructed geological history, as well as the identified fossil data, the Interbedded Sandstone–Claystone Unit is interpreted to be older than zones N10–N14 (Table 2). Next, the youngest rock unit, the Carbonate Sandstone Unit, is dated to zones N15–N18 (Table 3). As for the Diabase Intrusion, the age determination is based on the law of cross-cutting relationships, where this intrusive unit cuts through the Fragmented Claystone Unit and the Monomict Breccia Unit, which are considered to be of Middle Miocene age (Asikin, 1992) [1].

Table 1: Planktonic Fossils and the Age of the Monomict Breccia Unit (Blow, 1969)

Satuan	No Sampel	Bagian	KENOZOIKUM																							Foraminifera Planktonik
			Tersier																				Kuarter			
			Oligosen			Miosen														Pliosen			Pleistosen			
						Awal					Tengah						Akhir									
			Neogen (N)																							
			1	2	3	4	5	6	7	8	9	10	11	12	13	14	15	16	17	18	19	20	21	22	23	
Breksi Monomik	LP 58	Atas									-	-	-	-	-	-	-	-	-	-	-	-	-	-	-	*Orbulina universa* (d'Orbigny)
						-	-	-	-	-	-	-	-	-	-	-	-	-	-	-	-	-	-	-		*Globigerinoides obliquus* (Bolli)
										-	-															*Globigerinoides sicanus* (de Stefani) ?

Table 2: Planktonic Fossils and the Age of the Interbedded Sandstone–Claystone Unit (Blow, 1969)

Satuan	No Sampel	Bagian	KENOZOIKUM																							Foraminifera Planktonik
			Tersier																				Kuarter			
			Oligosen			Miosen														Pliosen			Pleistosen			
						Awal					Tengah						Akhir									
			Neogen (N)																							
			1	2	3	4	5	6	7	8	9	10	11	12	13	14	15	16	17	18	19	20	21	22	23	
Batupasir Selang Seling Batulempung	LP 69	Atas	-	-	-	-	-	-	-	-	-	-	-	-	-	-	-	-	-	-	-	-	-	-	-	*Orbulina universa* (d'Orbigny)
											-	-	-	-	-	-	-	-	-							*Globigerinoides obliquus* (Bolli)
														-	-	-	-	-	-	-	-	-	-	-	-	*Globorotalia merotumida* (Blow & Banner)
									-	-	-	-	-	-	-	-										*Globorotalia menardii* (Parker, Jones & Brady)
								-	-	-	-	-	-	-	-	-	-	-	-	-	-	-	-	-	-	*Globigerinoides seiglei* (Bermudez & Bolli)
	LP 119	Tengah	-	-	-	-	-	-	-	-	-	-	-	-	-	-	-	-	-	-	-	-	-	-	-	*Globigerinoides trilobus* (Reuss)
														-												*Globorotalia fohsi fohsi* (Kennett & Srinivasan)
						-	-	-	-	-	-	-	-	-	-	-	-	-	-	-	-	-	-	-		*Globigerinoides seiglei* (Bermudez & Bolli)
											-	-	-	-	-	-	-	-	-							*Globorotalia conoidea* (Walters)
														-	-	-	-	-	-	-	-	-	-	-	-	*Globorotalia menardii* (Parker, Jones & Brady)
	LP 58	Bawah										-	-													*Globigerinoides trilobus* (Reuss)
						-	-	-	-	-	-	-	-	-	-	-	-	-	-	-	-	-	-	-		*Globorotalia conoidea* (Walters)
						-	-	-	-	-	-	-	-	-	-	-	-									*Globorotalia menardii* (Parker, Jones & Brady)
			-	-	-	-	-	-	-	-	-	-	-	-	-	-	-	-	-	-	-	-	-	-	-	*Globigerina druryi* (Akers)
											-	-	-	-	-	-	-									*Globigerinoides immaturus* (LeRoy)

Table 3. Planktonic Fossils and the Age of the Carbonate Sandstone Unit (Blow, 1969)

Satuan	No Sampel	Bagian	KENOZOIKUM																							Foraminifera Planktonik
			Tersier																				Kuarter			
			Oligosen			Miosen														Pliosen			Pleistosen			
						Awal					Tengah						Akhir									
			Neogen (N)																							
			1	2	3	4	5	6	7	8	9	10	11	12	13	14	15	16	17	18	19	20	21	22	23	
Batupasir Karbonatan	LP 31	Atas									•	•	•	•	•	•	•	•	•	•	•	•	•	•	•	*Orbulina universa* (d'Orbigny)
						•	•	•	•	•	•	•	•	•	•	•	•	•	•	•	•	•	•	•		*Globigerinoides obliquus* (Bolli)
																		•	•	•						*Globorotalia merotumida* (Blow & Banner)
														•	•	•	•	•	•	•	•	•	•	•	•	*Globorotalia menardii* (Parker, Jones & Brady)
						•	•	•	•	•	•	•	•	•	•	•	•	•	•	•	•	•	•	•		*Globigerinoides seiglei* (Bermudez & Bolli)
	LP 60	Tengah									•	•	•	•	•	•	•	•	•	•	•	•	•	•	•	*Orbulina universa* (d'Orbigny)
																		•	•	•	•	•				*Neogloboquadrina acostaensis* (Blow)
								•	•	•	•	•	•	•	•	•	•	•	•	•	•	•	•	•	•	*Globigerinoides immaturus* (LeRoy)
																	•	•	•							*Globorotalia paralenguaensis* (Blow)
			•	•	•	•	•	•	•	•	•	•	•	•	•	•	•	•	•	•	•					*Globoquadrina venezuelana* (Hedberg)
	LP 71	Bawah					•	•	•	•	•	•	•	•	•	•	•	•								*Globoquadrina Altispira* (Cushman)
			•	•	•	•	•	•	•	•	•	•	•	•	•	•	•	•	•	•	•	•	•	•	•	*Globigerina trilobus* (Reuss)
							•	•	•	•	•	•	•	•	•	•	•	•	•	•						*Globoquadrina Dehiscens* (Chapman)
																	•	•	•							*Globorotalia Exilis* (Blow)

Determination of the Depositional Environment of Rock Units

The depositional environment is determined based on several types of data, including lithological characteristics, micropaleontological analysis, and relevant literature references. For the Fragmented Claystone Unit, the depositional environment could not be interpreted from micropaleontological analysis due to barren results (absence of microfossils). However, based on its lithological characteristics—which include mixed fragments of quartz, lithic materials, and igneous rocks such as basalt, and the local presence of conglomeratic blocks—this unit is interpreted as the result of submarine mass wasting or slumping (Safarudin, 1982 in Asikin *et al*., 1992) [1]. Therefore, it is inferred that this unit was deposited in a deep marine depositional environment, likely within the bathyal zone (Table 4).

Micropaleontological analysis of the Monomict Breccia Rock Unit could only be conducted on the upper part of the unit, as the other sections yielded barren results. Based on lithological characteristics, the lower part of the unit exhibits sedimentary structures such as graded bedding, parallel lamination, and ripple lamination. According to Bouma's sequence classification (1962) [4], these features indicate a turbidite depositional environment. Referring to the stratigraphic column and Walker's facies classification (1982), the lower part displays diagnostic features of Ta facies in breccia lithology, and Tb–Tc facies in interbedded sandstone, suggesting a mid-fan depositional setting interpreted as a mid-fan lobe channel system. In the middle part of the unit, the absence of Bouma structures and the dominance of coarsening-upward Monomict Breccia are interpreted as CGL facies, representing deposition within an upper fan channel fill system. Meanwhile, the upper part again exhibits Bouma Tb and Tc structures within sandstone, similar to the lower section, indicating a depositional environment within the mid-fan, particularly in a mid-fan lobe channel setting. Therefore, based on microfossil analysis and lithological characteristics, the Monomict Breccia Unit is interpreted to have been deposited in a submarine fan environment located within the outer neritic zone. (Figure 8)

The Interbedded Sandstone–Mudstone Rock Unit, based on the lithological characteristics observed in the lower and middle parts, exhibits sedimentary structures such as scour marks, parallel lamination, and convolute lamination. According to the Bouma sequence, these features indicate a depositional environment influenced by turbidity currents. Based on analysis and interpretation using Walker's classification (1978) [16], the middle and lower parts of the unit can be interpreted as part of a Smooth–Channelized Mid-Fan depositional system. In contrast, the upper part, which is characterized by thickening carbonate mudstone interbedded with sandstone and lacks identifiable sedimentary structures, is interpreted as belonging to a Lower Fan depositional system (Figure 9). Therefore, the overall depositional environment is interpreted as a submarine fan setting within the middle to outer neritic zone.

Table 4. Bathymetric determination of the Carbonate Sandstone Unit (Bandy, 1976).

Satuan	No Sampel	Bagian	Analisa Lingkungan Pengendapan							Foraminifera Benthonik
			Brackish	Marginal Marine	Shelf			Bathyal		
					Inner Shelf	Middle Shelf	Outer Shelf	Upper Bathyal	Lower Bathyal	
Batupasir Karbonatan	LP 31	Atas								*Eponides* (Montfort)
										Cassidulina (d'Orbigny)
	LP 60	Tengah								Eponides (Montfort)
										Pyrgo (d'Orbigny)
	LP 71	Bawah								*Eponides* (Montfort)

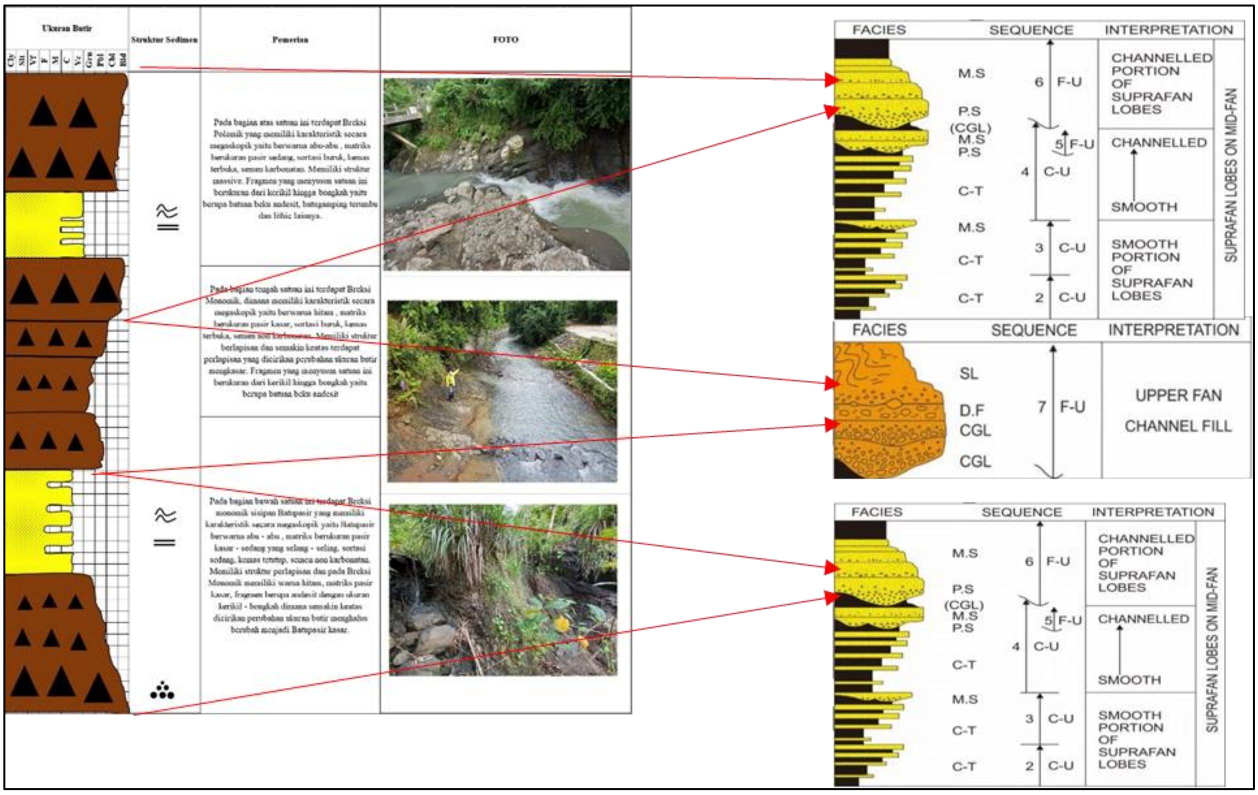

Fig 8: Interpretation of the depositional environment using Walker's 1978 classification.

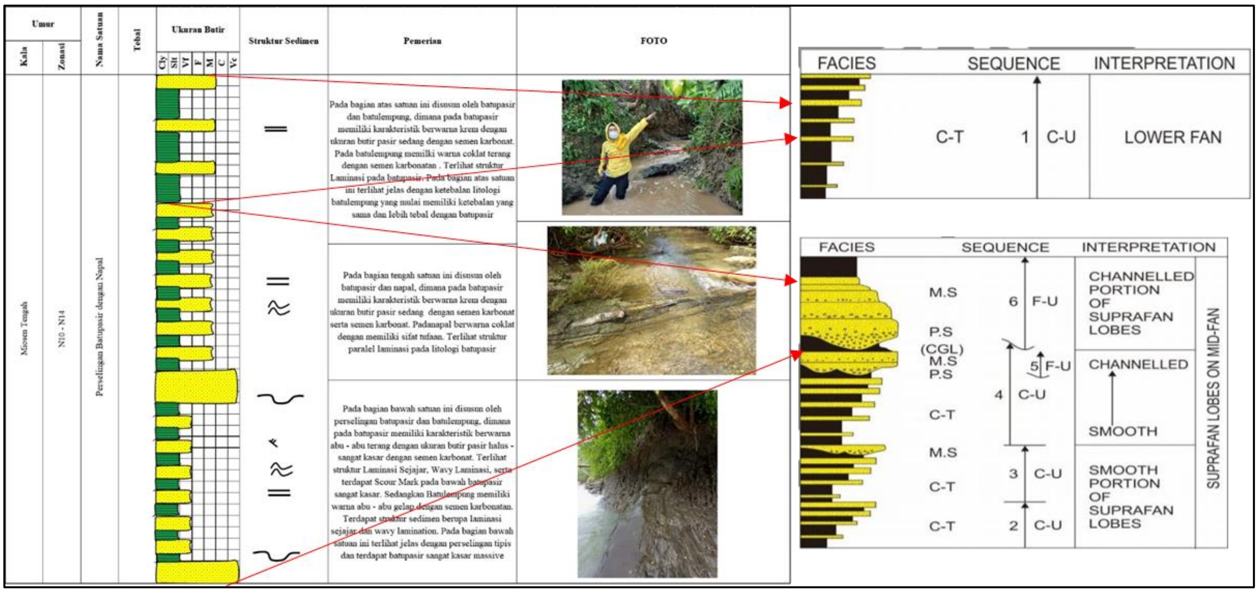

Fig 9: Depositional environment interpretation using Walker's 1978 [16] classification.

The Carbonate Sandstone Unit exhibits sedimentary structures characterized by massive sandstone at the base, transitioning upward into parallel lamination, wavy lamination, bedding, and an increasing abundance of rip-up mudrock structures. Based on facies modeling using the Bouma sequence (1962) [4], this unit is interpreted to have been deposited in a turbidite environment. Furthermore, based on the analysis of benthic fossils, the depositional setting is interpreted to be within the middle to outer neritic zone.

Furthermore, based on the characteristics of this unit as shown in Figure 10, it can be observed that thick massive sandstone is present, which can be classified as Facies B. Upward, it transitions into thinly bedded layers with sedimentary structures such as parallel lamination, wavy lamination, and the presence of rip-up mudrock structures, which are indicative of Facies A. These characteristics suggest a depositional environment associated with a Middle Fan Channel Fill System, as classified by Walker (1978) [16].

As for the diabase intrusion, the depositional environment interpretation of this intrusive unit is approached by observing the intrusion structures present in the field. The observed structures do not indicate that the intrusion occurred beneath the water surface, as there is no evidence of columnar jointing. Additionally, microscopic observation of this unit reveals a porphyritic texture, characterized by the presence of phenocrysts in the microscopic sample (F5) (Figure 7), which is indicative of a hypabyssal intrusive rock.

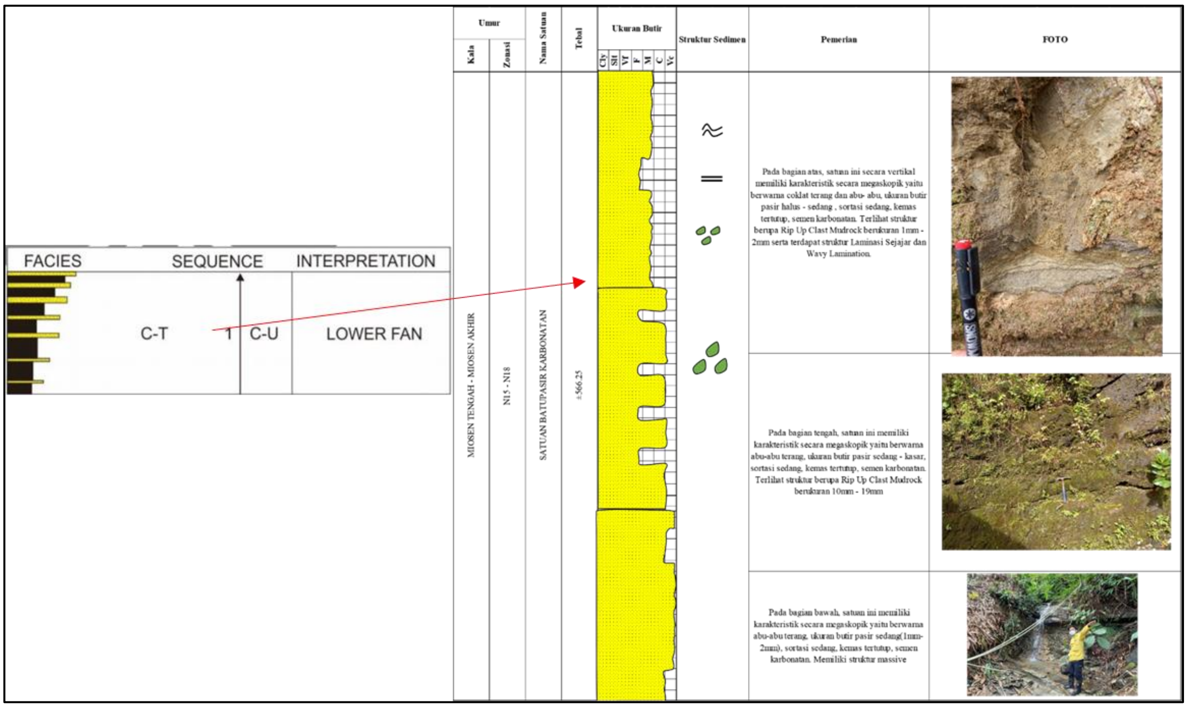

Fig 10: Depositional environment interpretation based on Walker's 1978 [16] classification.

Fig 11: Depositional environment interpretation based on Walker's 1978 [16] classification.

Structural Geology of the Study Area

In this study area, the geological structures were identified based on data obtained from measurements of joints in rocks, the strike and dip of rock layers, as well as the presence of offsets observed in outcrops. These structural indicators were correlated with contour patterns on a 1:12,500 scale topographic map, including linear hill alignments and abrupt river bends, to support the interpretation of geological structures within the research area.

The naming of geological structures in the study area is based on local geographic references, such as the names of villages and rivers where structural features were identified. The geological structures that influence the study area primarily consist of faults and folds, including four faults, one anticline, and one syncline, as follows:

1. Karanggayam Normal Fault

2. Sempudoyong Normal Fault
3. Pohkumbang Reverse Fault
4. Penimbun Sinistral Strike-Slip Fault
5. Karanggayam Anticline
6. Pohkumbang Syncline

Fold Structures

The fold structures identified in the study area include the Karanggayam Anticline and the Penimbun Syncline, both trending west–east. Based on field observations, a variation in dip was observed in the southern part of the area, where opposing dip directions indicate the presence of an anticline with a west–east axial orientation. The naming of the anticline is based on its location, as it extends across Karanggayam Subdistrict, and is composed of the Carbonate Sandstone Unit and the Interbedded Sandstone–Mudstone Unit.

Kinematic analysis yielded the following structural data:

- Limb 1: N 101° E / 30°
- Limb 2: N 271° E / 60°
- Hinge Surface: N 94° E / 75°
- Hinge Line: Plunge 4°, Trend N 273° E
- T1 (Principal stress direction 1): Plunge 24°, Trend N 04° E
- T2 (Principal stress direction 2): Plunge 04°, Trend N 273° E
- T3 (Principal stress direction 3): Plunge 73°, Trend N 164° E

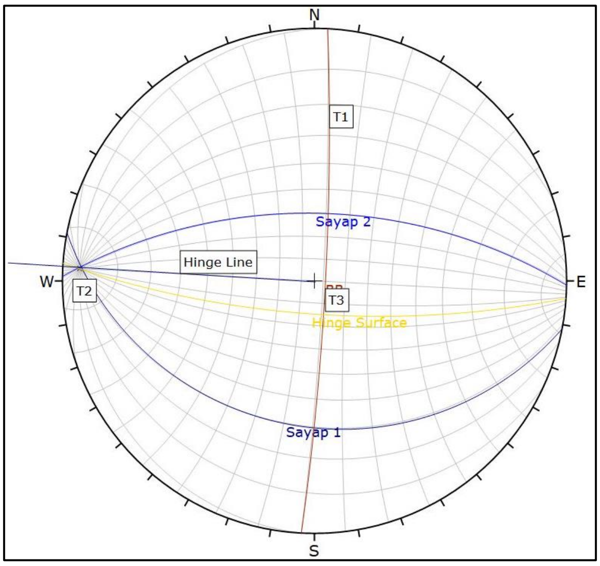

Fig 12: Kinematic Analysis of the Karanggayam Anticline

In addition, field observations revealed a change in dip orientation in the central part of the study area, where converging dips indicate the presence of a syncline with a west–east-trending axis. The naming of this syncline is based on its geographic location, extending across Karanggayam Subdistrict, and it is composed of the Interbedded Sandstone–Mudstone Unit.

Fault Stuctures

The fault structures identified in the study area include reverse faults, normal faults, and sinistral (left-lateral) strike-slip faults. The occurrence of these various fault types is closely related to regional tectonic activity. The island of Java has experienced at least three major tectonic regimes: an initial compressional phase, followed by an extensional phase, and later a return to a compressional regime. These tectonic events, in combination with lithological characteristics, have resulted in the development of diverse fault types.

In the southern part of the study area, based on observations of strike and dip, minor fault offsets, the presence of joints, fault scarps, and repetition of rock units within the Carbonate Sandstone Unit, a west–east-trending normal fault structure is interpreted. This normal fault is named after its location along Karanggayam Village, where it cuts through the Carbonate Sandstone Unit.

The following evidence supports the interpretation of this normal fault:

1. Layer Distribution Interpretation: The spatial distribution of the sandstone layers indicates that carbonate sandstone lithology is still present at lower contour levels beyond the fault scarp, where older lithologies should have been encountered. This suggests stratigraphic repetition caused by a normal fault.
2. Minor Fault Planes and Shear Fractures: Observations of minor fault surfaces and parallel shear fractures further support the occurrence of a normal fault.
3. Drag Fold Evidence: A drag fold observed at location LP 123 is interpreted as resulting from displacement along the normal fault.

Stereographic Analysis: Stereographic projection using shear and gash fracture data, combined with topographic lineaments and fault scarps, was used to determine the orientation and position of the Karanggayam normal fault plane.

Based on the geological analysis, the geological evolution of the study area can be summarized, including both its depositional and structural histories. Stratigraphic analysis indicates that sedimentation in the area occurred from the Middle Miocene to the Pliocene. The region's structural development has been strongly influenced by the tectonic regimes that have acted upon Java during and after these periods

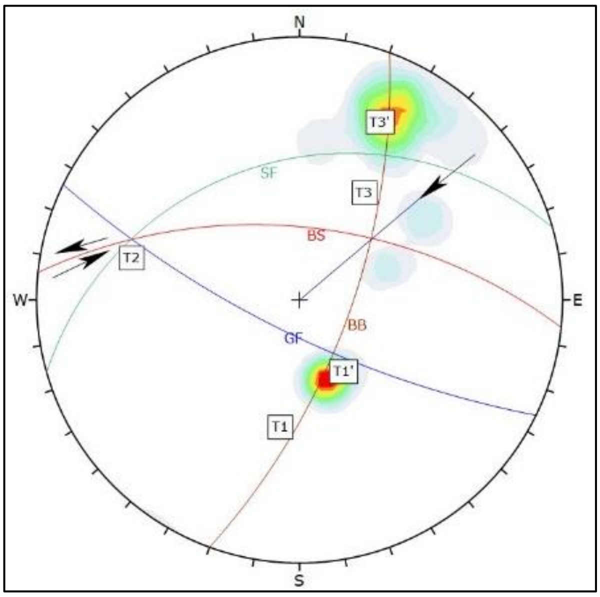

Fig 13: Kinematic Analysis of the Karanggayam Normal Fault

Analysis of this normal fault also included a kinematic analysis, resulting in the following data:

1. GF: N 116° E / 75°
2. SF: N 254° E / 34°
3. Plane T1 T2: N 20° E / 68°
4. Fault Plane: N 276° E / 59°
5. Rake: 50°
6. T1: 34°, N 184° E
7. T2: 21°, N 290° E
8. T3: 38°, N 39° E

Based on Rickard's (1972) classification, this fault is identified as a Left Normal Slip Fault.

In the central part of the field, based on observations of strike and dip, it is interpreted that there is a fault plane and joint sets, as well as a contour that is higher than the surrounding area, suggesting the presence of a thrust fault structure trending approximately west–east.

The naming of this normal fault is based on the location where it was found, namely from Pohkumbang Village to the Blebe River, where the fault cuts through the interbedded sandstone–mudstone unit. The interpretation of this thrust fault is supported by evidence of faulting, namely:

1. Interpretation of a contour higher than the surrounding area, indicating uplift in the central block.
2. The presence of a steep dip of 60–80°.
3. Interpretation of a crushed zone around the fault plane, thought to be the result of thrust faulting.
4. Stereographic analysis using fracture data in the form of shear fractures and gash fractures was employed to determine the lineaments that serve as references for the fault planes and to interpret the existing fault surfaces.

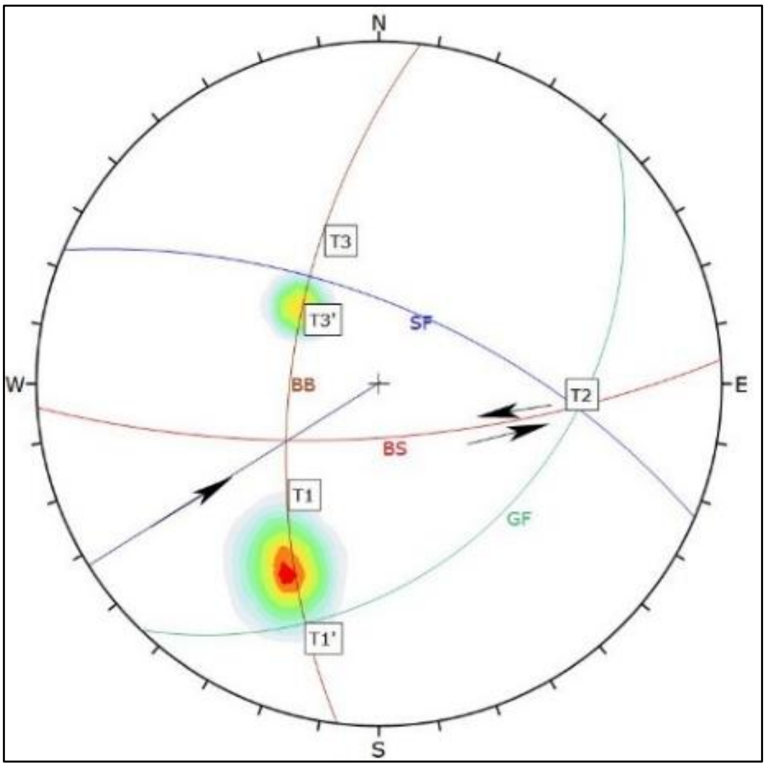

Fig 14: Kinematic Analysis of the Pohkumbang Thrust Fault

Attitude:

1. SF: N 293° E / 64°
2. GF: N 44° E / 35°
3. Plane T1 T2: N 187° E / 61°
4. Fault Plane: N 86° E / 72°
5. Rake: 54°
6. T1: 215°, N 41° E
7. T2: 29°, N 95° E
8. T3: 38°, N 341° E

Based on Rickard's (1972) classification, this fault is identified as a Right Reverse Slip Fault.

In the northern part of the field, based on observations of strike and dip, joint sets, and the presence of fault scarps in both sandstone and monomict breccia lithologies—interpreted as fault planes—it is concluded that there is a normal fault structure trending approximately west–east.

The naming of this normal fault is based on the location where it was identified, namely in the northeastern part of the Penimbun Village block. It is also interpreted that this normal fault extends westward across the block. This interpretation is supported by the following evidence:

Interpretation of linear contour features and fault scarps in the field, suggesting displacement due to normal faulting.Identification of a fault plane and, from a distance in the northwest of the block, interpretation of a triangular facet morphology.

Stereographic analysis using fracture data in the form of shear fractures and gash fractures, combined with the alignment of contours where the fault scarp is located, serving as a reference for defining the Penimbun normal fault plane.

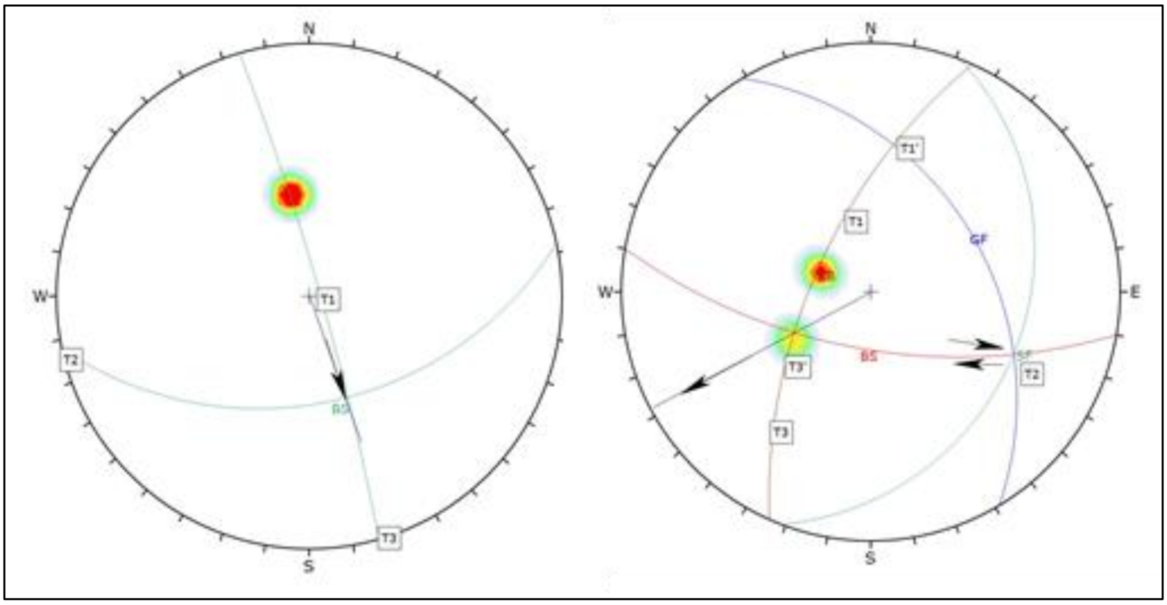

Fig 15: Kinematic Analysis of the Penimbun Normal Fault

There is also a fault structure that cuts across the entire field. Based on observations of strike and dip, offsets on minor faults, and joint sets found within the monomict breccia unit, the interbedded sandstone–mudstone unit, river lineament patterns, and irregular strike–dip measurements, it is interpreted that there is a sinistral (left-lateral) strike-slip fault trending approximately northeast–southwest.

The naming of this sinistral strike-slip fault is based on the location where it was identified, namely from Penimbun Village through Pohkumbang to Grenggeng, where the fault cuts through the fragmental mudstone unit, monomict breccia unit, interbedded sandstone–mudstone unit, and carbonate sandstone unit.

The following evidence supports the interpretation of this sinistral strike-slip fault:

1. Interpretation of the distribution of stratigraphic units showing non-matching contacts along the strike line, along with the presence of linear features (LP) indicating orientation influenced by this sinistral fault.
2. Interpretation of an observable offset consistent with sinistral fault movement.
3. Stereographic analysis using fracture data in the form of shear fractures and gash fractures, along with the interpretation of a fault plane and contour lineaments, was used as a reference for defining the Penimbun Sinistral Strike-Slip Fault plane.

The analysis of the sinistral strike-slip fault was also carried out using Dips 6.0 software for its kinematic analysis, resulting in the following data:

1. SF: N 339° E / 76°
2. GF: N 322° E / 56°
3. T1–T2 Plane: N 79° E / 56°
4. Fault Plane: N 184° E / 68°
5. Rake: 42°
6. T1: 18°, N 91° E
7. T2: 33°, N 346° E
8. T3: 14°, N 249° E

Based on Rickard's (1972) classification, this fault is categorized as a Normal Left Slip Fault.

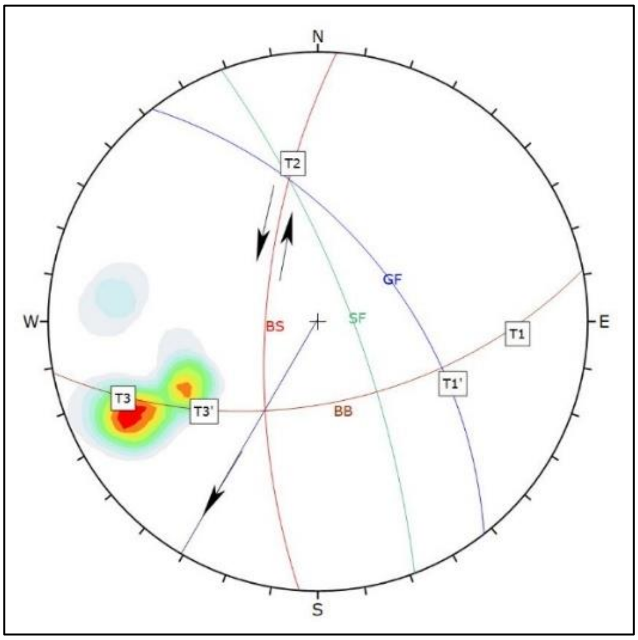

Fig 16: Kinematic Analysis of the Penimbun Sinistral Strike-Slip Fault

Historical Geology of the Field Area

Based on the analysis of the study area in terms of geomorphology, stratigraphy, and geological structure, the geological history of this region can be interpreted as a reconstruction from the earliest to the latest events. This geological history describes the sequence of deposition and the structural controls that influenced the study area. From stratigraphic and micropaleontological analyses, the depositional history of this area began in the Early Miocene and continued until the Late Miocene.

The geological history begins with the deposition of the Fragmental Claystone Unit, which formed in a deep marine environment and is older than N10 in age. This unit has lithological characteristics such as scaly structures, indicative of intense deformation processes at the time, and contains fragments. Based on its lithological characteristics, this unit can be correlated with the Karangsambung Formation according to the Geological Map of the Kebumen Sheet, Asikin *et al*. (1992) [1].

Following the deposition of the Fragmental Claystone Unit, volcanic disturbances and activity occurred, resulting in the formation of the Monomict Breccia Unit. This unit was deposited through a turbidity current process, characterized by specific lithological and sedimentary structures. The source material is interpreted to have originated from the north–northeast, as indicated by increasingly coarser fragments toward that direction. Based on lithological characteristics, this unit was deposited in an Upper Fan System – Mid Fan Lobe System (Walker, 1978) [16]. Microfossil analysis could only be conducted on the upper part of the Monomict Breccia Unit, indicating an outer neritic environment.

After this phase, a weakened zone formed, enabling diabase intrusions that cut through both the Fragmental Claystone and Monomict Breccia units. The diabase intrusion is characterized as an intermediate igneous rock with diabasic texture. The absence of well-formed hexagonal columns suggests that the intrusion occurred in the presence of water, preventing the formation of perfect columnar joints and resulting in irregular cooling structures (entablature). The age of this intrusion is estimated to be Early Miocene, as it cuts through the two previously deposited units.

As volcanic activity decreased, deposition resumed with the Interbedded Sandstone–Mudstone Unit, conformable with the previous units. This unit, dated to N10–N14, is interpreted to have been deposited by turbidity currents in a middle–outer neritic environment. Based on lithological characteristics, it was deposited in a Lower – Smooth to Channelized Mid Fan environment (Walker, 1978) [16].

Following this, volcanic activity continued to decline, leading to the deposition of the Carbonate Sandstone Unit, also conformable with the preceding unit. This unit is interpreted to have been deposited in a turbidite setting, as indicated by sedimentary structures that suggest a turbidite environment. Based on planktonic foraminiferal fossil determinations, its age is estimated to be Middle Miocene or older than N15–N18. Benthic foraminiferal analysis indicates deposition in a middle–outer neritic environment. According to Walker's (1978) [16] depositional environment classification, this unit corresponds to a Mid Fan Channel Fill System.

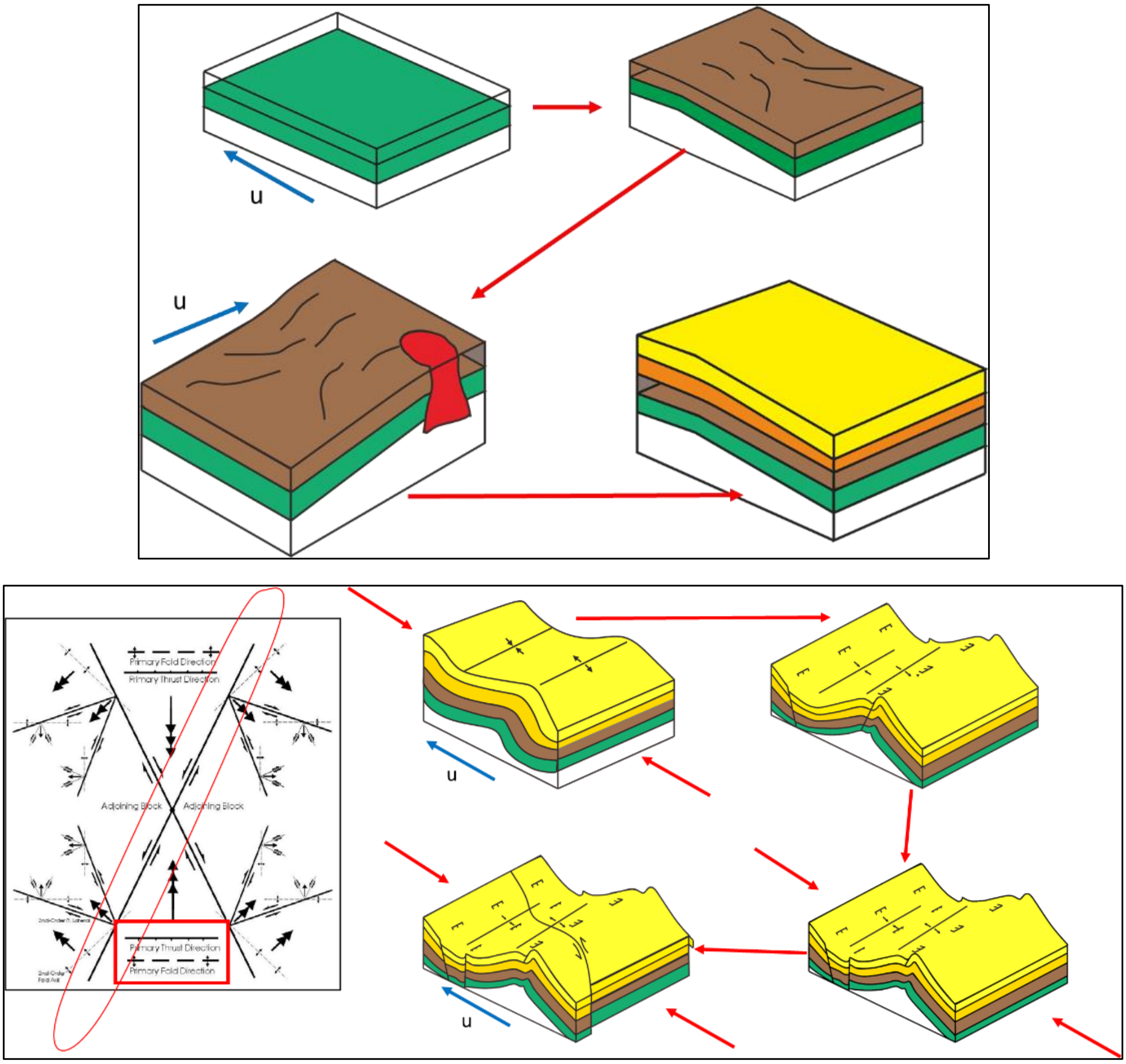

Fig 17: Depositional History Model of the Study Area

After all depositional processes were completed, in addition to erosion, a phase of geological deformation occurred. Due to north–south-oriented compressional forces, folds in the form of anticlines and synclines with east–west-trending axes were formed. Once the compression ended, a release phase occurred, resulting in the formation of a normal fault in the northern part of the area and near the folds within the field. This normal fault is interpreted to have formed when the rocks, having been strongly compressed, lost the compressional force holding them, causing them to collapse and produce normal faulting.

Subsequently, another tectonic phase took place, generating north–south-oriented compressional forces. This time, the deformation formed a thrust fault with an east–west-oriented axis. The thrust fault in this area is evident from bedding planes that dip almost vertically. This fault plane likely developed along bedding surfaces, as bedding planes are zones of weakness that can accommodate slip. As the compressional force increased further, a sinistral (left-lateral) strike-slip fault was formed, cutting across the previously developed geological structures (Figure 17). Throughout the formation of these structures, exogenic processes were also at work. These surface processes eroded the study area, progressively exposing outcrops and shaping the present-day land surface.

4. Conclusion

The study area, located in Karanggayam District, Kebumen Regency, Central Java Province—covering the villages of Karanggayam, Pohkumbang, Penimbun, and Karangmojo—consists of four lithostratigraphic units and one lithodemic unit arranged from oldest to youngest: the Fragmental Claystone Unit, the Monomict Breccia Unit, the Diabase Intrusion Unit, the Interbedded Sandstone–Mudstone Unit, and the Carbonate Sandstone Unit. Geological structures identified in the area include the Karanggayam Anticline, Penimbun Syncline, Karanggayam Normal Fault, Penimbun Normal Fault, Pohkumbang Thrust Fault, and Penimbun Sinistral Strike-Slip Fault. The geological history of the area is divided into two main phases: the depositional phase and the structural formation phase. Deposition occurred from the Early to Late Miocene in a submarine fan environment dominated by turbidity current processes, while the structural phase involved the development of various folds and faults after sedimentation. The diabase intrusion is interpreted to have formed during the Middle Miocene, as it cuts through the Monomict Breccia Unit.

5. Acknowledgements

This research was supported and guided by the Department of Geological Engineering, Faculty of Earth Technology and Energy, Universitas Trisakti.

References

1. Asikin S, Handoyo A, Busono H, Gafoer S. Peta Geologi Lembar Kebumen, Jawa. Bandung: Pusat Penelitian dan Pengembangan Geologi; 1992.
2. Nugroho B. Parameter Stadia Sungai dan Stadia Daerah. Jakarta: Jurusan Teknik Geologi, Fakultas Teknologi Mineral, Universitas Trisakti; 2000.
3. Bandy OL. Foraminiferal Indices in Paleoecology. Stratigraphic Geology Division; 1967.
4. Bouma A. Sedimentology of Some Flysch Deposits. Amsterdam: Elsevier Publishing Co.; 1962. 186 p.
5. Bramantyo B, Bandono. Klasifikasi Bentuk Muka Bumi (Landform) untuk Pemetaan Geomorfologi Skala 1:25.000 dan Aplikasinya untuk Penataan Ruang. Jurnal Geoaplika. 2006;1(2):71-8.
6. Fleuty MJ. The Description of Folds. Proc Geol Assoc. 1964;75:461-92.
7. Deigh C. Integrated reservoir characterization of deepwater turbidite systems: A systematic review of seismic attribute analysis, well log integration, and dynamic data validation, with a focus on the Niger Delta Fold Belt. Int J Multidiscip Res Growth Eval. 2024;5(6):1798-1814. doi:10.54660/IJMRGE.2024.5.6.1798-1814.
8. Howard AD. Drainage Analysis In Geologic Interpretation: A Summation. AAPG Bull. 1967;51(11):2246-59.
9. Kartanegara L, Uneputty H, Asikin S. Tatanan Stratigrafi dan Posisi Tektonik Cekungan Jawa Tengah Utara selama Jaman Tersier. In: Proceedings of PITIAGI ke-16; 1987; Bandung.
10. Lobeck AK. Geomorphology, An Introduction to the Study of Landscapes. New York: McGraw Hill Book Company, Inc.; 1939.
11. Moody JD, Hill MJ. Wrench Fault Tectonics. Bull Geol Soc Am. 1956;67:1207-46.
12. Pulunggono, Martodjojo S. Perubahan Tektonik Paleogene–Neogene Merupakan Peristiwa Tektonik Terpenting di Jawa. In: Proceeding Geologi dan Geotektonik Pulau Jawa. Yogyakarta: Percetakan Nafiri; 1994.
13. Rickard MJ. Classification of Translational Fault Slip. Geol Soc Am. 1972.
14. Verstappen HTh. Outline of Geomorphology of Indonesia. Enschede: ITC; 2000. 212 p.
15. Thornbury WD. Principles of Geomorphology. New York: John Wiley; 1969.
16. Varnes DJ. Slope Movement Types and Processes. In: Schuster RL, Krizek RJ, editors. Landslides, Analysis and Control. Washington, DC: National Academy of Sciences; 1978. p. 11-33. (Transportation Research Board, Special Report No. 176).
17. Walker RG. Deep-water Sandstone Facies and Ancient Submarine Fans: Model for Exploration for Stratigraphic Traps. AAPG Bull. 1978;62(6):932-66.